Communications in Mathematics and Applications
Vol. 15, No. 5, pp. 1525–1540, 2024
ISSN 0975-8607 (online); 0976-5905 (print)
Published by RGN Publications
DOI: 10.26713/cma.v15i5.2851

http://www.rgnpublications.com

Research Article

Approximate Analytical Study on a System of Non-Linear Partial Differential Equations in Chemical Science

B. Sathyapriya, V. Ananthaswamy* and J. Anantha Jothi

Research Centre and PG Department of Mathematics, The Madura College (Affiliated to Madurai Kamaraj University), Madurai, Tamil Nadu, India
***Corresponding author:** ananthu9777@gmail.com

Received: August 12, 2024 **Accepted:** December 3, 2024

Abstract. Within a biofilter filled coupled with the woodchip-compost-blend, the biofiltration of mixtures containing toluene as well as *n*-propanol is discussed in this study. The chemical oxidation actions occurring within the gas and also biofilm phases, as well as the distribution of mass across the biofilm surface form the basis of the model's structure. By employing a new homotopy perturbation approach, the semi-analytical outcomes for the *n*-propanol and toluene concentrations in non-dimensional form for the two phases have been found under time-dependent conditions for all appropriate experimental values of the parameters. Additionally, this study provides the MATLAB programming, which is employed as a numerical simulation for the problem. Through numerical simulation, the derived semi-analytical results are verified. The effects of several variables, such as non-dimensional constants for time-dependent conditions, are illustrated graphically.

Keywords. Mathematical modelling, Toluene, *n*-Propanol, Non-linear boundary value problem, New Homotopy Perturbation Method (NHPM), Numerical simulation

Mathematics Subject Classification (2020). 35B20, 35C20, 35G31, 35J05

1. Introduction

Numerous research works have concentrated on issues brought about by the atmospheric release of gaseous effluents that comprise *Volatile Organic Compounds* (VOCs). These investigations have resulted in the creation of other bioreactors in more recent decades, including the bioscrubber, biofilter, as well as biotrickling filter. As a possible substitute for traditional

air pollution reduction techniques, biofiltration has gained recognition. However, because to the difficulty of characterising the underlying phenomena and the absence of internationally recognised physical, chemical, and biological factors, gas biofilter representing has lagged behind experimental research in terms of development.

According to Dorado *et al*. [8] ten wrapping substances employed in biofiltration have undergone extensive characterisation. To have a better understanding of their benefits and limitations, data was contrasted and reviewed. Organic materials, particularly composted and coconut fibres, have demonstrated the ability to maintain adequate water content for microbes and to eventually deliver inorganic nutrients. As a result of Rene *et al*. [17] shows that benzene is successfully removed at the stage of vapour by a microbial consortium relying on a composted biofilter. Delhoménie *et al*. [5] report regarding the findings of a three-month experimental investigation conducted at the laboratory scale upon the biofiltration processing for toluene-contaminated air. *Methyl Isobutyl Ketone* (MIBK), a volatile chemical molecule that is thought to be extremely poisonous, is the subject of Raghuvanshi and Babu [16] research on biofiltration. For two months, the biofiltration experiment was conducted in a lab setting employing an acclimated mixed culture. When Shareefdeen and Baltzis [20] used numerical methods to solve the model equations for biofiltration of toluene vapour; the projected concentration profiles of both transient and steady-state operation closely matched the actual data. Krishnakumar *et al*. [13] examined the biofilter bed's overall effectiveness in terms of pollutant removal as well as sustainability. Deshusses *et al*. [6] have created and discussed a novel diffusion response framework for the estimation of steady-state as well as transient-state performance regarding biofilters for the biotreatment of waste air. The model was applied by Martin *et al*. [15] and integrated into the accessible software package Biofilter. Thin-fibre membrane bioreactors may successfully remove combinations of toluene and n-hexane vapours, as demonstrated by Zhao *et al*. [24]. These complex biological connections may have an impact on one or more for the pollutants being treated in gas-phase membrane bioreactors. Furthermore, it provides more confirmation of the hollow fibre membrane bioreactors' promising potential for treating toxic air streams. Fan *et al*. [9] state that the biofilm's density and place of origin exert an enormous influence on how the substrate diffuses onto the biofilm. Beyenal and A. Tanyolaç [4] came to the conclusion that the biofilm density fluctuates and that the active and then observable biofilm thicknesses may differ when a biofilm reactor is in operation. Alvarez-Hornos *et al*. [1] presented a dynamic framework for the biofiltration-based extraction of toluene and ethyl acetate.

Dorado *et al*. [8] work examines and contrasts ten packing materials that frequently serve as media for support at biofiltration to determine which ones are most appropriate based on certain physical attributes. Delhoménie *et al*. [5] reports on the findings of a three-month experimental investigation conducted within the laboratory level on the biofiltration processing of toluene-contaminated air. Deshusses *et al*. [6] have given and analysed an experimental assessment of a novel framework for the explanation of gaseous waste biofiltration.

The main purpose of this work is to utilize NHPM for attaining the approximate analytical results for the mixtures of non-dimensional concentrations for toluene and n-propanol in the gas phase and biofilm phase. The approximate analytical results and the numerical simulations are finally compared, along with a graphical representation. To discuss the effects of various non-dimensional constants and factors on the non-dimensional concentrations of mixtures including toluene and n-propanol in the gas phase and biofilm phase, graphical illustrations are provided.

2. Mathematical Formulation of the Problem

The ability of the biofilter to reduce the amounts of toluene and *n*-propanol was assessed via a mathematical model. The model, which outlines the essential steps in biofiltration, including diffusion, convection, biodegradation, and absorption is significantly altered by Deshusses *et al*. [6]. Utilising cross-inhibition impacts of the substrate–pollutant combination, the researchers employed Monod-type processes. In deriving the regulating equations, the following premises are considered.

- The biofilm/air dividing factor represents the equilibrium over the gas-biofilm interface.
- There cannot be biodegradation taking place inside the pores of the adhering particles because the biofilm exists solely on their exterior surfaces.
- As a result, the thickness for the biofilm is significantly more than a solid's size support; planar biofilm geometry is employed to make model equations.
- Now, there is not any more a gas-phase boundary layer over the air/biofilm contact. Consequently, it is possible to disregard the gas-phase mass exchange barrier.
- There is no overabundance of biomass accumulation, and the characteristics for biomass, which include particular areas of surface, kinetic coefficients, and thickness, are uniform across the filter bed.
- Only *n*-propanol, as well as toluene, acts as substrates that change the process of biodegradation.

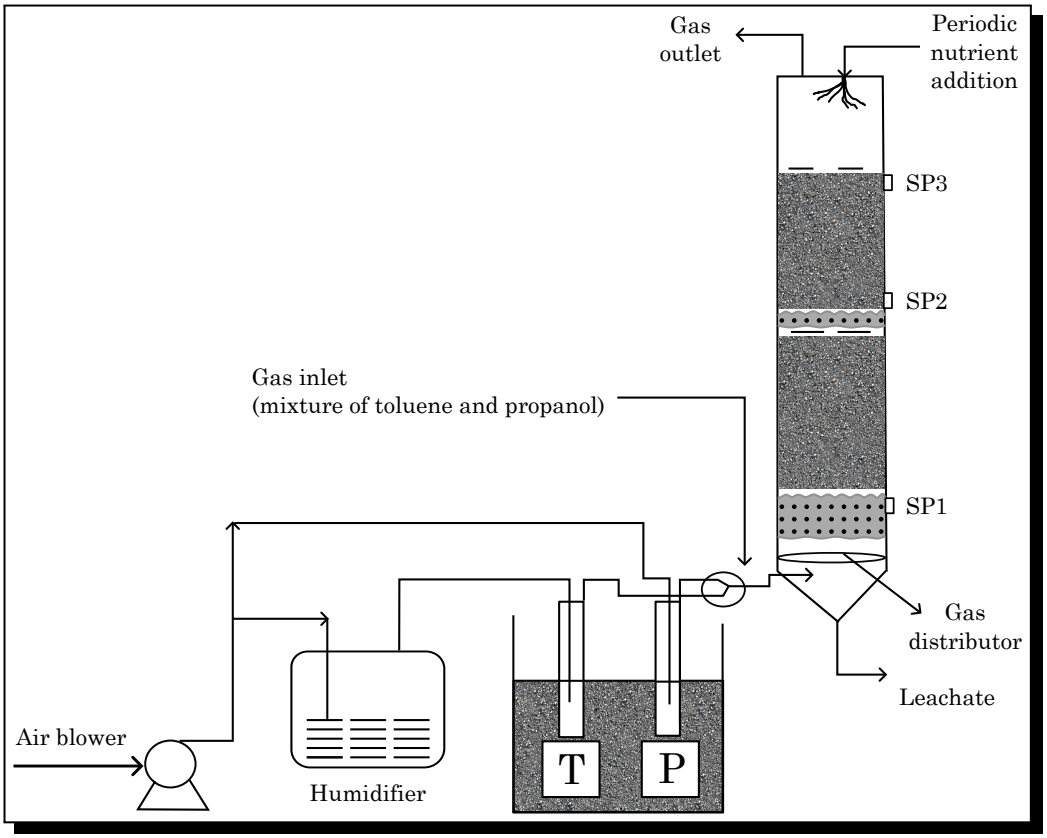

Figure 1. Schematic diagram for (sampling ports, toluene, propanol); *n*-propanol had been employed exclusively in toluene and *n*-propanol combined studies [7]

2.1 Mass Balance at the Biofilm Phase

The following are the differential equations in non-linear for extracting a combination of toluene and n-propanol from a biofilter (Dixit *et al*. [7]):

$$\frac{\partial S_t}{\partial t} = D_{et}\frac{\partial^2 S_t}{\partial x^2} - \mu_{\max(t)}\frac{X}{Y_{\frac{x}{s}}}\frac{S_t(x)}{K_S + S_t(x) + \frac{(S_p(x))^2}{K_i}}, \tag{2.1}$$

$$\frac{\partial S_p}{\partial t} = D_{ep}\frac{\partial^2 S_p}{\partial x^2} - \mu_{\max(p)}\frac{X}{Y_{\frac{x}{s}}}\frac{S_p(x)}{K_S + S_p(x)}. \tag{2.2}$$

The respective initial and boundary conditions are as follows:

$$\text{At } t = 0,\ S_t = S_p = 0,\ 0 \le x \le \delta, \tag{2.3}$$

$$\text{At } t < 0,\ S_t = \frac{c_t}{m_t},\ S_p = \frac{c_p}{m_p},\ x = 0, \tag{2.4}$$

$$\text{At } t < 0,\ \frac{\partial S_t}{\partial x} = \frac{\partial S_p}{\partial x} = 0,\ x = \delta, \tag{2.5}$$

where $S_p(x)$, $S_t(x)$ denotes the propanol, toluene concentration's, and D_{et}, D_{ep} represents the effective diffusivity for toluene and propanol at the biofilm, X is the dry cell density of the biofilm, K_t is an inhibition constant, K_S indicates the half saturation constant of toluene, $\mu_{\max(t)}$ and $\mu_{\max(p)}$ are maximum particular pace while toluene and propanol biodegradation, $Y_{\frac{x}{s}}$ is the yield coefficient of biomass, m_t and m_p are the partition coefficient of the toluene and propanol within the biofilm and δ represents the biofilm thickness.

2.2 Mass Balance at Air Phase

The mass balance equations for the concentrations of toluene and propanol in the air phase are as follows:

$$\varepsilon\frac{\partial C_t}{\partial t} = U_g\frac{\partial C_t}{\partial h} - a_s D_{et}\left[\frac{\partial S_t}{\partial x}\right]_{x=0}, \tag{2.6}$$

$$\varepsilon\frac{\partial C_p}{\partial t} = U_g\frac{\partial C_p}{\partial h} - a_s D_{ep}\left[\frac{\partial S_p}{\partial x}\right]_{x=0}. \tag{2.7}$$

The respective initial conditions are as follows:

$$\text{At } h = 0,\ C_t = C_{ti},\ C_p = C_{pi}, \tag{2.8}$$

where i indicates the concentration for the respective *volatile organic compound* (VOCs) at the inlet for the biofilter, and C_p, C_t denotes the concentration for the propanol, toluene within the air stream, H represents the height of the bed at biofilter, ε indicates the porosity of the bed, and a_s represents the surface area for the biofilm.

2.3 Non-Dimensional Form for Mass Balance at the Biofilm Phase and Air Phase

To simplify equations (2.1)-(2.8) into a non-dimensional form, the following non-dimensional parameters are introduced:

$$\left.\begin{aligned} &\chi = \tfrac{x}{\delta},\ P = \tfrac{S_t C_t}{m_t},\ R = \tfrac{S_p C_p}{m_p},\ \varphi_1 = \mu_{\max(t)}\tfrac{X\delta^2}{Y_{\frac{x}{s}} D_{et} K_s},\ \varphi_2 = \mu_{\max(p)}\tfrac{X\delta^2}{Y_{\frac{x}{s}} D_{ep} K_s},\\ &\alpha_1 = \tfrac{c_t}{m_t K_s},\ \alpha_2 = \left(\tfrac{c_p}{m_p}\right)^2\tfrac{1}{K_s K_i},\ \alpha_3 = \tfrac{c_p}{m_p K_s},\ \lambda = \tfrac{H a_s D_{et}}{U_g \delta c_{ti}},\ \lambda_1 = \tfrac{H a_s D_{ep} S_p}{U_g \delta c_{pi}},\\ &Z = \tfrac{h}{H},\ A = \tfrac{c_t}{c_{ti}},\ B = \tfrac{c_p}{c_{pi}} \end{aligned}\right\}. \tag{2.9}$$

By utilizing the above non-dimensional parameters in equations (2.1)-(2.8), we attained the non-dimensional form for mass balance equations at the biofilm phase

$$\frac{\partial P}{\partial \tau} = \frac{\partial^2 P}{\partial \chi^2} - \frac{\varphi_1 P(\chi)}{1+\alpha_1 P(\chi)+\alpha_2 (P(\chi))^2}, \tag{2.10}$$

$$\frac{\partial R}{\partial \tau} = \frac{\partial^2 R}{\partial \chi^2} - \frac{\varphi_2 R(\chi)}{1+\alpha_3 R(\chi)} = 0, \tag{2.11}$$

where $P(\chi)$, $R(\chi)$ indicates the non-dimensional concentration of toluene and n-propanol φ_1, φ_2, α_1, α_2, α_3 are non-dimensional constant, χ is the non-dimensional distance, τ is the non-dimensional time.

The initial and boundary conditions for the aforementioned equations are as follows:

$$\text{At } \tau,\ \chi = 0,\ P = 1,\ R = 1, \tag{2.12}$$

$$\text{At } \chi = 1,\ \frac{\partial P}{\partial \chi} = 0,\ \frac{\partial R}{\partial \chi} = 0. \tag{2.13}$$

Non-dimensional form of mass balance equations at the air phase is given by

$$\frac{dA}{dZ} = \lambda \left[\frac{dP}{d\chi}\right]_{\chi=0}, \tag{2.14}$$

$$\frac{dB}{dZ} = \lambda_1 \left[\frac{dR}{d\chi}\right]_{\chi=0}. \tag{2.15}$$

The respective boundary conditions are

$$Z = 0,\ \ A = \frac{c_t}{c_{ti}},\ \ B = \frac{c_p}{c_{pi}}, \tag{2.16}$$

where A, B denotes the non-dimensionless concentration for toluene, n-propanol at air stream, Z denotes the non-dimensional height, λ, λ_1 are the non-dimensional constant.

3. Approximate Analytical Results for the Non-Linear Differential Equations by Utilizing New Homotopy Perturbation and Laplace Transform Techniques

Differential equations, both non-linear and linear, can be used to simulate a wide range of activities and have a significant impact on many scientific and technical disciplines. The analytical solutions are inappropriate for a large number of differential equations in non-linear form. Some semi-analytical techniques that can be utilized for accurately resolving differential equations in non-linear which are variational Iterative technique (Wazwaz [22]), new homotopy perturbation technique (Ananthaswamy *et al*. [2,3]), homotopy analysis technique (Beyenal and Tanyolaç [4], and Sajid and Hayat [18]), Akbari-Ganji technique (Seethalakshmi *et al*. [19]).

The *Homotopy Perturbation Technique* (HPM) was developed by He [10–12] to produce approximate analytical results. One of the easiest and most effective method to obtain an approximate analytical solution for non-linear differential equation is HPM. The effective application of homotopy perturbation approach is to solve the initial and boundary value problems. The perturbation strategy is based on the assumption that there are few parameters. The semi-analytical formulas obtained by perturbation techniques may be appropriate across little values of minor parameters because of the vast number of non-linear situations. Perturbation solutions are frequently as successful when the scientific system's parameters

are very small. The approximation cannot be fully relied upon because there are no guidelines for the presence of minor parameters. As such, analytical and experimental confirmation of the approximation's accuracy is crucial. Recently, HPM has been suggested as a solution to these problems. After that, He [11] uses unique approaches based on the homotopy perturbation technique to resolve the differential equations which are in non-linear at the zeroth iteration called *New Homotopy Perturbation Technique* (NHPM).

3.1 Approximate Analytical Outcomes for the Concentration Equations at Biofilm Phase

By employing the new homotopy perturbation technique, laplace transform technique (Ananthaswamy *et al*. [2, 3]), we were able to get the time-dependent solutions to equations (2.10) and (2.11).

We generate the homotopy shown below for equation (2.10) and (2.11):

$$(1-p)\left[\frac{\partial^2 P}{\partial \chi^2}-\frac{\varphi_1 P(\chi)}{1+\alpha_1 P(\chi)+\alpha_2 (P(\chi))^2}-\frac{\partial P}{\partial \tau}\right]+p\left[\frac{\partial^2 P}{\partial \chi^2}-\frac{\varphi_1 P(\chi)}{1+\alpha_1 P(\chi)+\alpha_2 (P(\chi))^2}-\frac{\partial P}{\partial \tau}\right]=0, \tag{3.1}$$

$$(1-p)\left[\frac{\partial^2 R}{\partial \chi^2}-\frac{\varphi_2 R(\chi)}{1+\alpha_3 R(\chi)}-\frac{\partial R}{\partial \tau}\right]+p\left[\frac{\partial^2 R}{\partial \chi^2}-\frac{\varphi_2 R(\chi)}{1+\alpha_3 R(\chi)}-\frac{\partial R}{\partial \tau}\right]=0. \tag{3.2}$$

By applying NHPM in above equations (3.1)-(3.2), we get

$$(1-p)\left[\frac{\partial^2 P}{\partial \chi^2}-\frac{\varphi_1 P(\chi)}{1+\alpha_1+\alpha_2}-\frac{\partial P}{\partial \tau}\right]+p\left[\frac{\partial^2 P}{\partial \chi^2}-\frac{\varphi_1 P(\chi)}{1+\alpha_1+\alpha_2}-\frac{\partial P}{\partial \tau}\right]=0, \tag{3.3}$$

$$(1-p)\left[\frac{\partial^2 R}{\partial \chi^2}-\frac{\varphi_2 R(\chi)}{1+\alpha_3}-\frac{\partial R}{\partial \tau}\right]+p\left[\frac{\partial^2 R}{\partial \chi^2}-\frac{\varphi_2 R(\chi)}{1+\alpha_3}-\frac{\partial R}{\partial \tau}\right]=0. \tag{3.4}$$

Equations (3.3)-(3.4) have approximate analytical solutions that are

$$P=P_0+pP_1+p^2P_2+\ldots, \tag{3.5}$$

$$R=R_0+pR_1+p^2R_2+\ldots. \tag{3.6}$$

Substituting the equations (3.5) and (3.6) in equations (3.3) and (3.4), then comparing the coefficients of p^0, we attained

$$p^0:\frac{\partial^2 P_0}{\partial \chi^2}-\frac{\varphi_1 P_0(\chi)}{1+\alpha_1+\alpha_2}-\frac{\partial P_0}{\partial \tau}=0, \tag{3.7}$$

$$p^0:\frac{\partial^2 R_0}{\partial \chi^2}-\frac{\varphi_2 R_0(\chi)}{1+\alpha_3}-\frac{\partial R_0}{\partial \tau}=0. \tag{3.8}$$

The respective boundary conditions are

$$\text{At } \tau,\ \chi=0,\ P_0=1,\ R_0=1,\ P_i=R_i=0,\ i=1,2,3,\ldots, \tag{3.9}$$

$$\text{At } \chi=1,\ \frac{\partial P_i}{\partial \chi}=0,\ \frac{\partial R_i}{\partial \chi}=0,\ i=1,2,3,\ldots. \tag{3.10}$$

Now by applying laplace transform to the equation (3.7) to (3.10), we get

$$\frac{\partial^2 \overline{P_0}}{\partial \chi^2}-\frac{\varphi_1 \overline{P_0(\chi)}}{1+\alpha_1+\alpha_2}-\frac{\partial \overline{P_0}}{\partial \tau}=0, \tag{3.11}$$

$$\frac{\partial^2 \overline{R_0}}{\partial \chi^2}-\frac{\varphi_2 \overline{R_0(\chi)}}{1+\alpha_3}-\frac{\partial \overline{R_0}}{\partial \tau}=0, \tag{3.12}$$

$$\text{At } \tau,\ \chi = 0,\ \overline{P_0} = \frac{1}{S},\ \overline{R_0} = \frac{1}{S},\ P_i = R_i = 0,\ i = 1,2,3,\ldots \tag{3.13}$$

$$\text{At } \chi = 1,\ \overline{\frac{\partial P_i}{\partial \chi}} = 0,\ \overline{\frac{\partial R_i}{\partial \chi}} = 0,\ i = 1,2,3,\ldots \tag{3.14}$$

Solving equation (3.11) by using equations (3.13) and (3.14), we get

$$\overline{S_0} = \frac{\cosh\left(\sqrt{\frac{\varphi_1}{1+\alpha_1+\alpha_2}}\right)(1-\chi)}{S\cosh\left(\sqrt{\frac{\varphi_1}{1+\alpha_1+\alpha_2}}\right)} \tag{3.15}$$

Let's now analyse the equation (3.15) using a *Complex Inversion Formula* (CIF).

The *CIF* $y(t) = \frac{1}{2\pi i}\oint_c \exp(st)\overline{y}(s)ds$ defines $s = x + iy$, hence integration along lines $s = c$ within the complex plane is required if a function $y(t)$ is characterised by $\overline{y}(s)$ using laplace transform. The real number c is set so that $s = c$ seems to be right of each singularity, even though it should be random. In addition to the contour integral shown on the right hand for the equation, the integral in perform is examined utilising the so-called Bromwich contours. We use the residue theorem to compute the contour integrals for these analytic functions,

$$\oint_c F(z)dz = 2\pi i \sum_m \text{Res}[F(z)]_{z=z_0}. \tag{3.16}$$

Somewhere at the poles for function where the residues are computed $F(z)$. As a result, we notice in equation (3.17) that

$$y(t) = \sum_m \text{Res}[\exp[st]\overline{y}(s)]_{s=s_0}. \tag{3.17}$$

For complex variables, we could observe that the residue for a function $F(z)$ at a simple pole for $z = b$ is provided by the fundamental idea.

$$\text{Res}[F(z)]_{s=b} = \lim_{z\to b}\{(z-b)F(z)\}. \tag{3.18}$$

By employing *CIF* $\int_{\gamma-i\infty}^{\gamma+i\infty} e^{s\tau}U_0(\chi,t) = \frac{1}{2\pi i}\int_{\gamma-i\infty}^{\gamma+i\infty} e^{s\tau}\overline{U_0}(\chi,s)ds =$ the total of their contributions made by the integrand's poles.

To modify an equation (3.15), we must compute

$$\text{Res}\left(\frac{\cosh\left(\sqrt{\frac{\varphi_1}{1+\alpha_1+\alpha_2}}\right)(1-\chi)}{S\cosh\left(\sqrt{\frac{\varphi_1}{1+\alpha_1+\alpha_2}}\right)}\right).$$

By determining the poles of $\overline{S_0}$, we can observe that there exists a pole at and an infinite quantity of poles $s_m = -(2m+1)^2\frac{\pi^2}{4}$, where $m = 1,2,3,\ldots$.

Therefore, we have

$$L^{-1}(\overline{S_0}) = \text{Res}\left(\frac{\cosh\left(\sqrt{\frac{\varphi_1}{1+\alpha_1+\alpha_2}}\right)(1-\chi)}{S\cosh\left(\sqrt{\frac{\varphi_1}{1+\alpha_1+\alpha_2}}\right)}\right)_{s=0} + \text{Res}\left(\frac{\cosh\left(\sqrt{\frac{\varphi_1}{1+\alpha_1+\alpha_2}}\right)(1-\chi)}{S\cosh\left(\sqrt{\frac{\varphi_1}{1+\alpha_1+\alpha_2}}\right)}\right)_{s=s_m}. \tag{3.19}$$

Equation (3.19) has the first residue as follows:

$$\text{Res}\left(\frac{\cosh\left(\sqrt{\frac{\varphi_1}{1+\alpha_1+\alpha_2}}\right)(1-\chi)}{S\cosh\left(\sqrt{\frac{\varphi_1}{1+\alpha_1+\alpha_2}}\right)}\right)_{s=0} = \lim_{s\to 0}\frac{d}{ds}e^{s\tau}\left(\frac{\cosh\left(\sqrt{\frac{\varphi_1}{1+\alpha_1+\alpha_2}}\right)(1-\chi)}{S\cosh\left(\sqrt{\frac{\varphi_1}{1+\alpha_1+\alpha_2}}\right)}\right) \tag{3.20}$$

$$= \frac{\cosh\left(\sqrt{\frac{\varphi_1}{1+\alpha_1+\alpha_2}}\right)(1-\chi)}{\cosh\left(\sqrt{\frac{\varphi_1}{1+\alpha_1+\alpha_2}}\right)}. \tag{3.21}$$

Equation (3.19) has the second residue as follows:

$$\operatorname{Res}\left(\frac{\cosh\left(\sqrt{\frac{\varphi_1}{1+\alpha_1+\alpha_2}}\right)(1-\chi)}{S\cosh\left(\sqrt{\frac{\varphi_1}{1+\alpha_1+\alpha_2}}\right)}\right)_{s=s_m} = \lim_{s\to s_m} e^{s\tau}\left(\frac{\cosh\left(\sqrt{\frac{\varphi_1}{1+\alpha_1+\alpha_2}}\right)(1-\chi)}{S\frac{d}{ds}\cosh\left(\sqrt{\frac{\varphi_1}{1+\alpha_1+\alpha_2}}\right)}\right) \tag{3.22}$$

$$= 16\sum_{m=0}^{\infty} \frac{\cos\left(\frac{2m+1}{2}\pi\left(1-\chi\right)\right)e^{-\left(\frac{\varphi_1}{1+\alpha_1+\alpha_2}+\frac{(mn+1)^2\pi^2}{4}\right)\tau}}{\left(\pi^2(2m+1)^2+4\left(\frac{\varphi_1}{1+\alpha_1+\alpha_2}\right)\right)(2m+1)\pi\sin\left(\frac{(2m+1)}{2}\pi\right)}. \tag{3.23}$$

By adding equations (3.21) and (3.23), we get

$$P(\chi) = \frac{\cosh\left(\sqrt{\frac{\varphi_1}{1+\alpha_1+\alpha_2}}\right)(1-\chi)}{\cosh\left(\sqrt{\frac{\varphi_1}{1+\alpha_1+\alpha_2}}\right) + 16\sum_{m=0}^{\infty}\frac{\cos\left(\frac{2m+1}{2}\pi(1-\chi)\right)e^{-\left(\frac{\varphi_1}{1+\alpha_1+\alpha_2}+\frac{(2m+1)^2\pi^2}{4}\right)\tau}}{\left(\pi^2(2m+1)^2+4\left(\frac{\varphi_1}{1+\alpha_1+\alpha_2}\right)\right)(2m+1)\pi\sin\left(\frac{(2m+1)}{2}\pi\right)}}. \tag{3.24}$$

The above equation is the approximate analytical outcomes for the non-dimensional concentration of toluene $P(\chi)$ in biofilm phase.

In similar manner, we can solve the equation (3.12), we get

$$R(\chi) = \frac{\cosh\left(\sqrt{\frac{\varphi_2}{1+\alpha_3}}\right)(1-\chi)}{\cosh\left(\sqrt{\frac{\varphi_2}{1+\alpha_3}}\right)} + 16\sum_{m=0}^{\infty}\frac{\cos\left(\frac{2m+1}{2}\pi(1-\chi)\right)e^{-\left(\frac{\varphi_2}{1+\alpha_3}+\frac{(2m+1)^2\pi^2}{4}\right)\tau}}{\left(\pi^2(2m+1)^2+4\left(\frac{\varphi_2}{1+\alpha_3}\right)\right)(2m+1)\pi\sin\left(\frac{(2m+1)}{2}\pi\right)}. \tag{3.25}$$

The above equation is the semi-analytical expressions for the non-dimensional concentration of n-propanol $R(\chi)$ in biofilm phase.

3.2 Approximate Analytical Outcomes for the Concentration Equations at Air Phase

The approximate analytical result for the non-dimensional concentration of toluene at the air phase is (Shareefdeen *et al*. [21], and Zarook and Shaikh [23]),

$$A(Z) = 1 - \eta Z\left(\frac{\varphi_1}{1+\alpha_1+\alpha_2}\right)\tanh\left(\frac{\varphi_1}{1+\alpha_1+\alpha_2}\right). \tag{3.26}$$

The approximate analytical outcome for the non-dimensional concentration of $n-$propanol at the air phase is (Shareefdeen *et al*. [21], and Zarook and Shaikh [23]),

$$B(Z) = 1 - \eta_1 Z\left(\frac{\varphi_2}{1+\alpha_3}\right)\tanh\left(\frac{\varphi_2}{1+\alpha_3}\right). \tag{3.27}$$

4. Numerical Simulation

The accuracy of our approximate analytical results for differential equations with non-linearity can be validated via numerical simulation (MATLAB). MATLAB functions pdepe are employed in the equations (2.10) and (2.11) which is given in Appendix A. As can be seen in Figures 1–6, when our approximate analytical expressions are compared to the numerical simulation, they are in good agreement.

5. Results and Discussions

Equations (3.24) and (3.25) are the approximate analytical results for non-dimensional concentrations of toluene and n-propanol in biofilm phase under time dependent by employing new homotopy perturbation technique.

Figures 1a–1c displays the time-dependent non-dimensional toluene concentration $P(\chi)$ against non-dimensional distance χ in the biofilm phase by utilizing equation (3.24). Figure 1a illustrates that the non-dimensional concentration of toluene $P(\chi)$ falls, the values of the non-dimensional constant φ_1 increase. As seen in Figures 1b and 1c, the non-dimensional concentration $P(\chi)$ rises as the values of the non-dimensional constants α_1, α_2 grow.

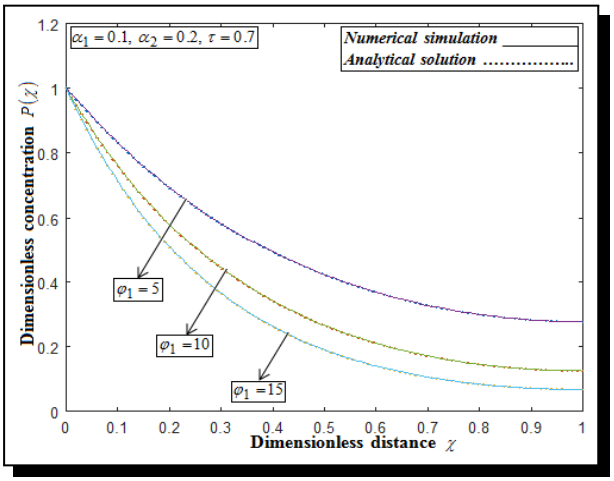

(a) Effects of non-dimensional constant φ_1 in non-dimensional concentration of toluene $P(\chi)$

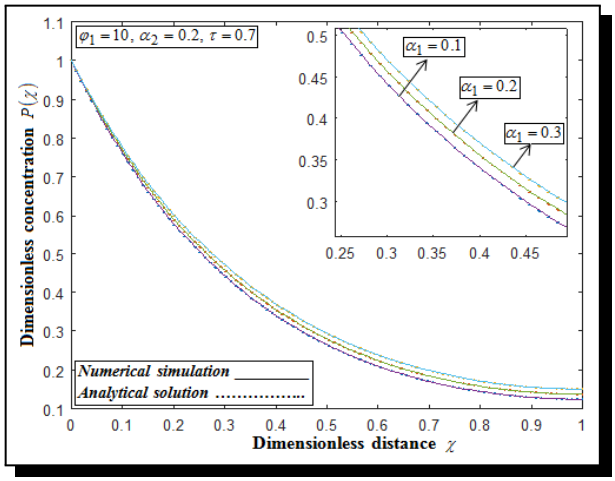

(b) Impacts of non-dimensional constant α_1 in non-dimensional concentration of toluene $P(\chi)$

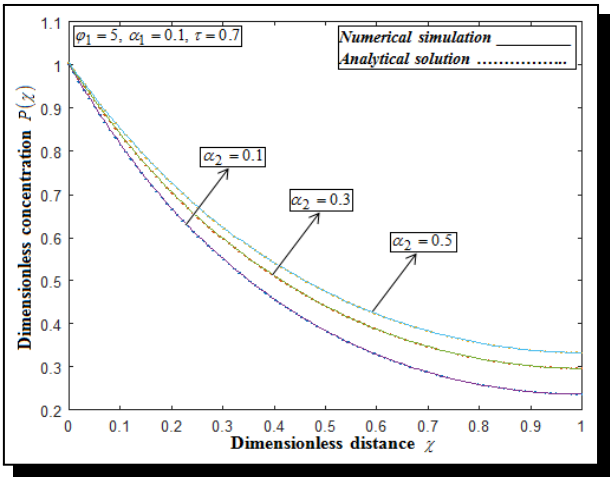

(c) Variations of non-dimensional constant α_2 in non-dimensional concentration of toluene $P(\chi)$

Figure 1

Figures 2a and 2b exhibits that the non-dimensional concentration of n-propanol $R(\chi)$ versus non-dimensional distance χ in gas phase under time-dependent by employing equation (2.4). As we can see in Figure 2a, the non-dimensional constant φ_1 values rise while the non-dimensional propanol $R(\chi)$ concentration falls. According to Figure 2b, when the non-dimensional constant α_3 values rise, so does the non-dimensional concentration.

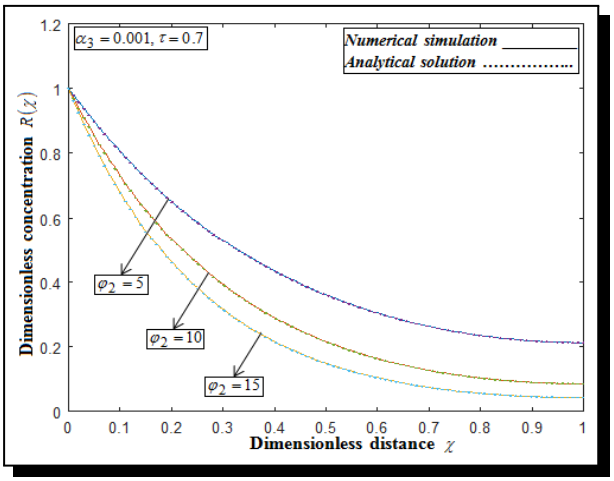

(a) Influence of non-dimensional constant φ_2 in non-dimensional concentration of n-propanol $R(\chi)$

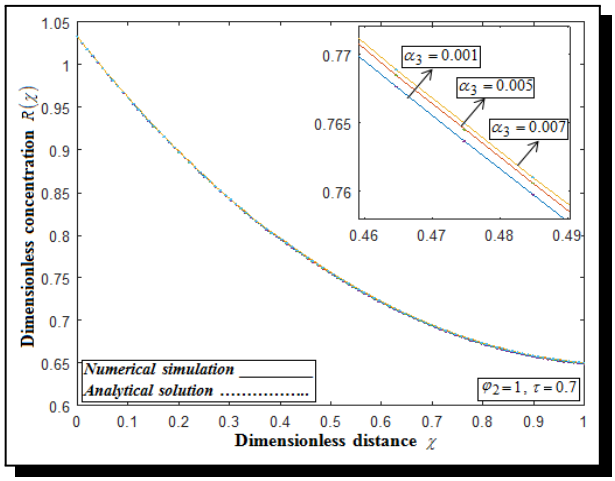

(b) Effect of non-dimensional constant α_3 in non-dimensional concentration of n-propanol $R(\chi)$

Figure 2

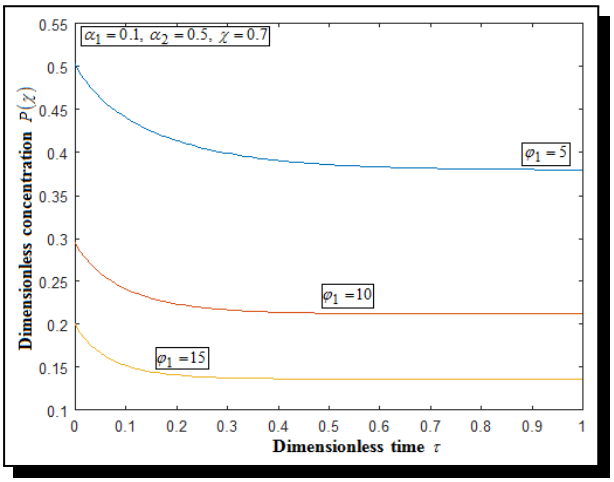

(a) Impact of non-dimensional constant φ_1 in non-dimensional concentration of toluene $P(\chi)$

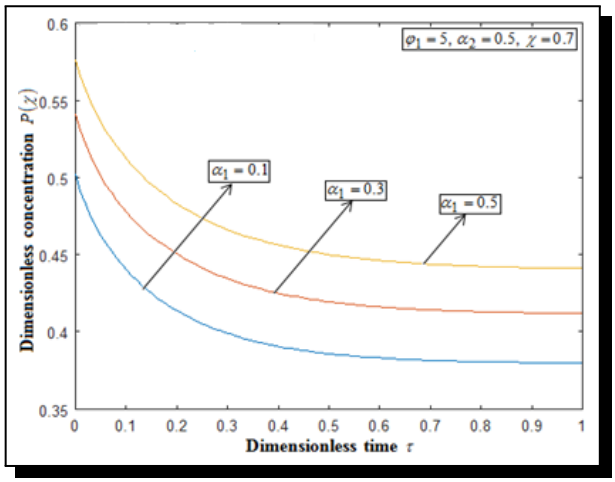

(b) Variation of non-dimensional constant α_1 in non-dimensional concentration of toluene $P(\chi)$

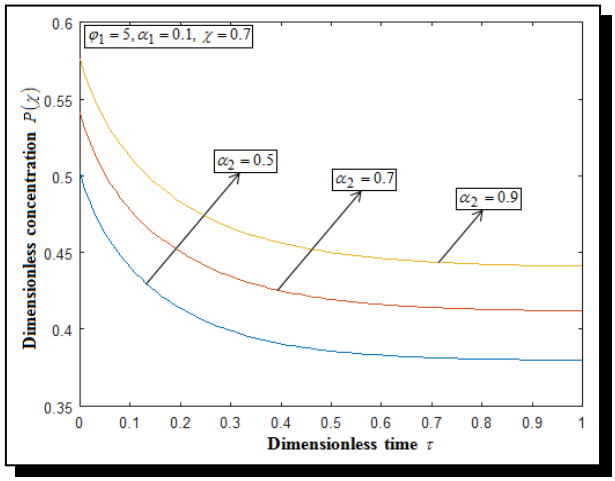

(c) Influence of non-dimensional constant α_2 in non-dimensional concentration of toluene $P(\chi)$

Figure 3

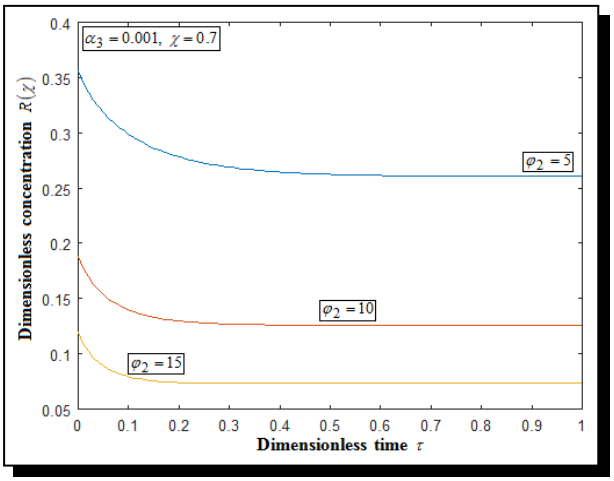

(a) Effect of non-dimensional constant φ_2 in non-dimensional concentration of n-propanol $R(\chi)$

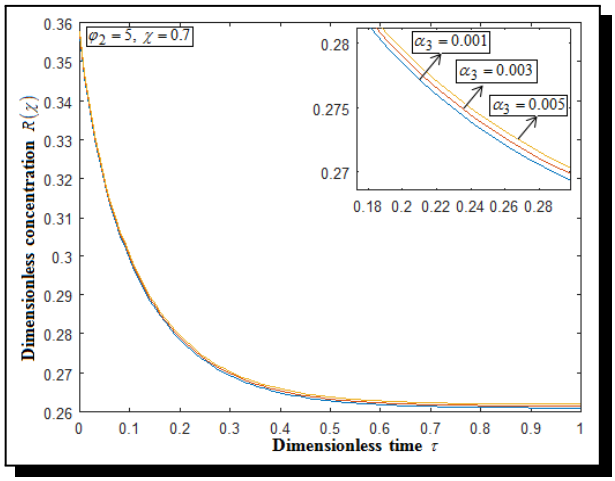

(b) Impact of non-dimensional constant α_3 in non-dimensional concentration of n-propanol $R(\chi)$

Figure 4

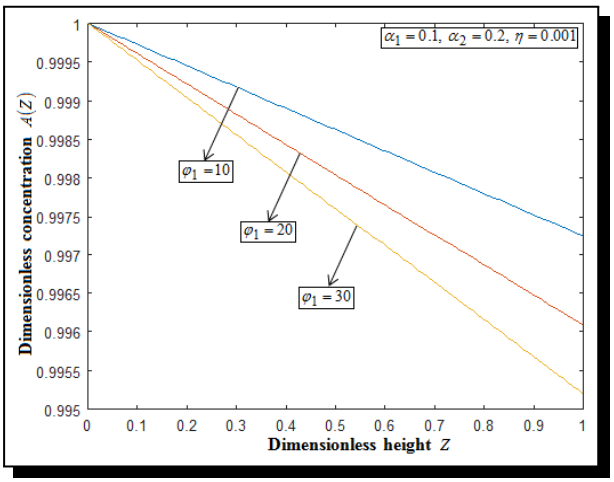

(a) Variation of non-dimensional constant φ_1 in non-dimensional concentration of toluene $A(Z)$

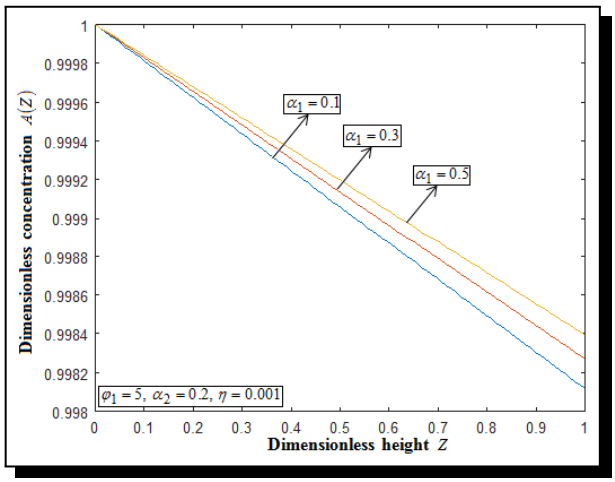

(b) Influence of non-dimensional constant α_1 in non-dimensional concentration of toluene $A(Z)$

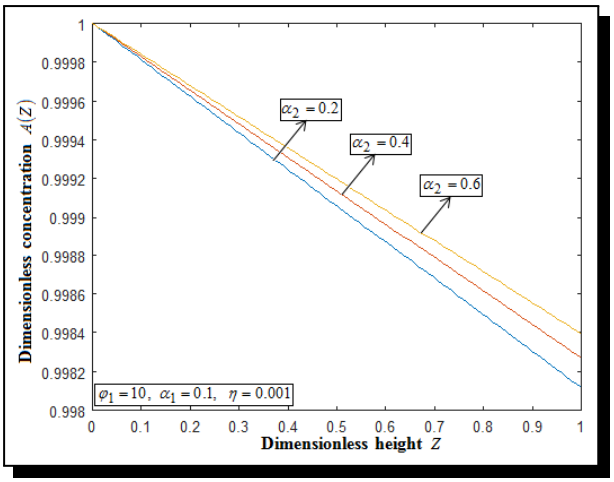

(c) Effect of non-dimensional constant α_2 in non-dimensional concentration of toluene $A(Z)$

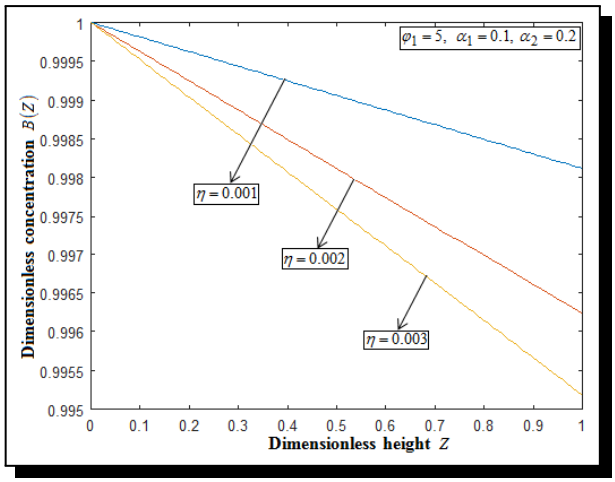

(d) Impact of non-dimensional constant η in non-dimensional concentration of toluene $A(Z)$

Figure 5

Figures 3a–3c exhibit that the non-dimensional concentration of toluene $P(\chi)$ versus non-dimensional time τ in biofilm phase under time-dependent by utilizing equation (3.24). As we can see in Figure 3a, the non-dimensional constant φ_1 values rises then the non-dimensional toluene $P(\chi)$ concentration get drops. Figures 3b and 3c depicts that, when the amount of non-dimensional constant α_1, and α_2 get rise, so does the non-dimensional concentration.

Figures 4a and 4b exhibit the non-dimensional concentration of n-propanol $R(\chi)$ versus non-dimensional time τ in gas phase under time-dependent by employing equation (2.4). From Figure 4a we observe that the non-dimensional propanol $R(\chi)$ concentration falls when the values of non-dimensional constant φ_2 values rise. In Figure 4b, when the non-dimensional constant α_3 values rise, so does the non-dimensional concentration.

Figures 5a–5c display the non-dimensional concentration of toluene $P(\chi)$ versus non-dimensional height Z at the air phases by employing equation (3.26). Figures 5a and 5d illustrate that the amount of non-dimensional constant φ_1 and η values rises then the non-dimensional concentration falls. In Figures 5b and 5c, the non-dimensional constant α_1 and α_2 values rise; also, the non-dimensional concentration gets increases.

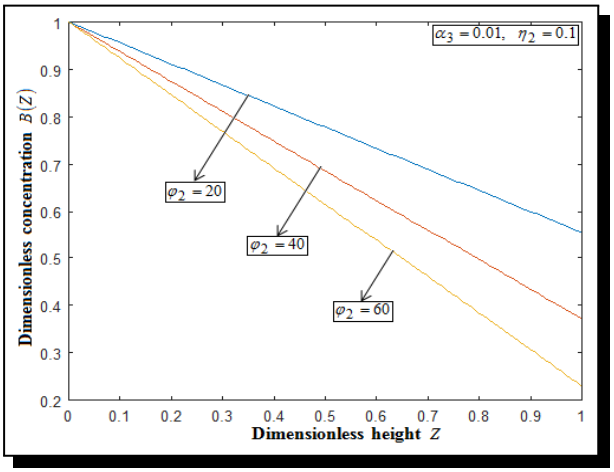

(a) Variation of non-dimensional constant ϕ_2 in non-dimensional concentration of n-propanol $B(Z)$

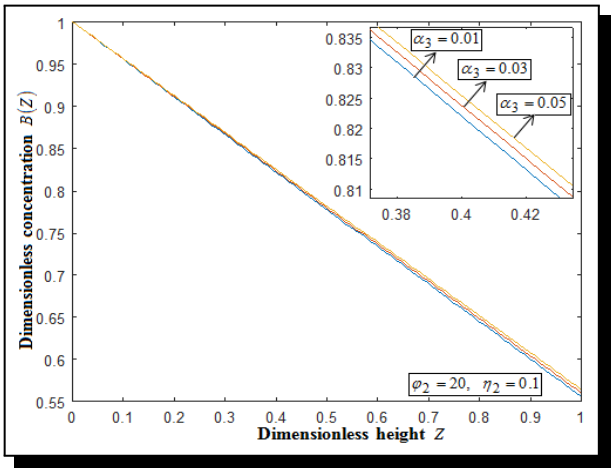

(b) Influence of non-dimensional constant α_3 in non-dimensional concentration of n-propanol $B(Z)$

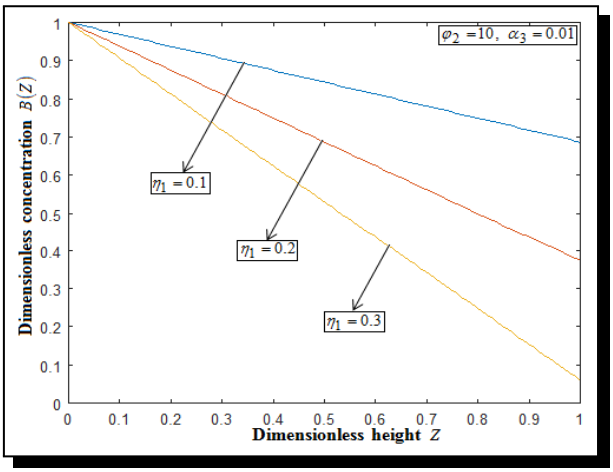

(c) Influence of non-dimensional constant η_1 in non-dimensional concentration of n-propanol $B(Z)$

Figure 6

Figures 6a–6c demonstrates that the non-dimensional concentration of n-propanol $R(\chi)$ versus non-dimensional height Z at the air phase by employing equation (3.27). Figures 6a and 6c show that, by increasing the amounts of non-dimensional constants φ_2 and η_1, then the non-dimensional concentration get drops. Figures 6b, the non-dimensional constant α_3 value raises also the non-dimensional concentration get increases.

6. Conclusion

The non-dimensional concentrations for toluene and n-propanol at the gas phase and biofilm phase under time-dependent conditions were resolved analytically by employing the new homotopy perturbation and Laplace techniques. Also, our approximate analytical results were compared with numerical simulation. The new homotopy perturbation technique yields even more accurate findings that closely resemble those of the numerical simulation. Graphical representations were used to show the effects of various parameters, namely non-dimensional constants for time-dependent. The researchers should be able to see how different parameters affect concentration with the help of the approximate analytical results exerted under the time dependent. The subsequent conclusions were arrived:

- The non-dimensional concentration of toluene and n-propanol versus non-dimensional time drops as the amounts of the non-dimensional constants φ_1, φ_2 rises.
- The non-dimensional concentrations of n-propanol and toluene against non-dimensional time grow as the values of the non-dimensional constants $\alpha_1, \alpha_2, \alpha_3$ rise.
- By increasing the amounts of non-dimensional constants $\varphi_1, \varphi_2, \eta, \eta_1$ then the non-dimensional concentration toluene and n-propanol at both biofilm phase and gas phase against the non-dimensional height Zget decreases.
- By raising the quantities of non-dimensional constants $\alpha_1, \alpha_2, \alpha_3$ so does the non-dimensional concentration toluene and n-propanol at both biofilm phase and gas phase against the non-dimensional height Z.

Appendix A: MATLAB Programming for Equations (2.10) and (2.11)

```
functionpdepe
M=0;
x=linspace(0,1);
t=linspace(0,1);
sol=pdepe(M,@pdex4pde,@pdex4ic,@pdex4bc,x,t);
v1=sol(:,:,1);
v2=sol(:,:,2);
%
figure
plot(x,v1(end,:))
title('v1(x,t)')
xlabel('Distance x')
ylabel('v1(x,1)')
%
figure
plot(x,v2(end,:))
title('v2(x,t)')
xlabel('Distance x')
```

```
ylabel('v2(x,2)')
%
function[c,f,s]=pdex4pde(x,t,v,DvDx)
c=[1;1];
f=[1;1].*DvDx;
P1=1;P2=1;A1=1;A2=1;A3=0.01;
F1=-P1*v(1)/(1+A1*v(1)+A2*v(2)^2);
F2=-P2*v(2)/(1+A3*v(2));
s=[F1;F2];
%
function v0=pdex4ic(t) %create an initial conditions
v0=[1;1];
%
function [Pl,Ql,Pr,Qr]=pdex4bc(xl,vl,xr,vr,t) %create a boundary conditions
Pl=[vl(1)-1;vl(2)-1];
Ql=[0;0];
Pr=[0;0];
Qr=[1;1];
```

Appendix B: Nomenclature

Symbols	Meaning
A	Non-dimensional concentration of toluene at air stream
a_s	Surface area of biofilm in the biofilter per unit volume
B	Non-dimensional concentration of n-propanol at the air stream
C_{pi}, C_{ti}	Concentration for n-propanol as well as toluene at the inlet air stream
h	Dimension height for the biofilters
H	Total height for the biofilters
K_p, K_t	Monod kinetics for n-propanol and toluene in half saturation constant
C_t, C_p	Concentrations for toluene and n-propanol in the air stream
K_i	Monod kinetics in inhibition constant
m_t, m_p	Non-dimensional partition coefficients for toluene and n-propanol at air film
S_t, S_p	Concentrations of toluene and n-propanol in the biofilm
U_g	Superficial velocity of air over the biofilter
D_{ep}, D_{et}	Diffusivity effective for n-propanol and toluene within the biofilm
x	Depth coordinate at the biofilm
X	Biofilm dry cell density
χ	Non-dimensional depth coordinate in the biofilm
P, R	Non-dimensional concentrations for toluene and n-propanol at the biofilm
$Y_{\frac{x}{s}}$	Biomass yield coefficient
Z	Non-dimensional height
$\varphi_1, \varphi_2, \alpha_1, \alpha_2, \alpha_3, \eta, \eta_1$	Non-dimensional constants
ε	Non-dimensional porosity for the filter bed

Symbols	**Meaning**
δ	Biofilm thickness
$\mu_{\max}$	Maximum specific growth rate of toluene degraders

Competing Interests

The authors declare that they have no competing interests.

Authors' Contributions

All the authors contributed significantly in writing this article. The authors read and approved the final manuscript.

References

[1] F. J. Álvarez-Hornos, C. Gabaldón, V. Martínez-Soria, P. Marzal and J.-M. Penya-roja, Mathematical modeling of the biofiltration of ethyl acetate and toluene and their mixture, *Biochemical Engineering Journal* **43**(2) (2009), 169 – 177, DOI: 10.1016/j.bej.2008.09.014.

[2] V. Ananthaswamy and S. Narmatha, Mathematical analysis of reversible inhibitor biosensor systems in dynamic mode, *Singapore Journal of Scientific Research* **10**(3) (2020), 229 – 265, DOI: 10.3923/sjsres.2020.229.265.

[3] V. Ananthaswamy, J. Chitra, J. A. Jothi and S. Sivasundaram, A mathematical study on non-linear initial-boundary value problem for R-D equation, *Nonlinear Studies* **31**(1) (2024), 327 – 351.

[4] H. Beyenal and A. Tanyolaç, Simultaneous evaluation of effective diffusion coefficients of the substrates in a biofilm with a novel experimental method, *The Canadian Journal of Chemical Engineering* **74**(4) (1996), 526 – 533, DOI: 10.1002/cjce.5450740413.

[5] M.-C. Delhoménie, L. Bibeau, N. Bredin, S. Roy, S. Broussau, R. Brzezinski, J. Kugelmass and M. Heitz, Biofiltration of air contaminated with toluene on a compost-based bed, *Advances in Environmental Research* **6**(3) (2002), 239 – 254, DOI: 10.1016/s1093-0191(01)00055-7.

[6] M. A. Deshusses, G. Hamer and I. J. Dunn, Behavior of biofilters for waste air biotreatment. 1. Dynamic model development, *Environmental Science & Technology* **29**(4) (1995), 1048 – 1058, DOI: 10.1021/es00004a027.

[7] R. M. Dixit, S. C. Deshmukh, A. A. Gadhe, G. S. Kannade, S. K. Lokhande, R. A. Pandey and M. A. Deshusses, Treatment of mixtures of toluene and *n*-propanol vapours in a compost–woodchip-based biofilter, *Environmental Technology* **33**(7) (2012), 751 – 760, DOI: 10.1080/09593330.2011.592226.

[8] A. D. Dorado, F. J. Lafuente, D. Gabriel and X. Gamisans, A comparative study based on physical characteristics of suitable packing materials in biofiltration, *Environmental Technology* **31**(2) (2010), 193 – 204, DOI: 10.1080/09593330903426687.

[9] L.-S. Fan, R. Leyva-Ramos, K. D. Wisecarver and B. J. Zehner, Diffusion of phenol through a biofilm grown on activated carbon particles in a draft-tube three-phase fluidized-bed bioreactor, *Biotechnology and Bioengineering* **35**(3) (2004), 279 – 286, DOI: 10.1002/bit.260350309.

[10] J.-H. He, Homotopy perturbation method: a new nonlinear analytical technique, *Applied Mathematics and Computation* **135**(1) (2003), 73 – 79, DOI: 10.1016/S0096-3003(01)00312-5.

[11] J.-H. He, Homotopy perturbation technique, *Computer Methods in Applied Mechanics and Engineering* **178**(3-4) (1999), 257 – 262, DOI: 10.1016/s0045-7825(99)00018-3.

[12] J.-H. He, Some asymptotic methods for strongly nonlinear equations, *International Journal of Modern Physics B* **20**(10) (2006), 1141 – 1199, DOI: 10.1142/S0217979206033796.

[13] B. Krishnakumar, A. M. Hima and A. Haridas, Biofiltration of toluene-contaminated air using an agro by-product-based filter bed, *Applied Microbiology and Biotechnology* **74** (2007), 215 – 220, DOI: 10.1007/s00253-006-0641-x.

[14] S. Liao and A. Campo, Analytic solutions of the temperature distribution in Blasius viscous flow problems, *Journal of Fluid Mechanics* **453** (2019), 411 – 425, DOI: 10.1017/S0022112001007169.

[15] R. W. Martin Jr., H. Li, J. R. Mihelcic, J. C. Crittenden, D. R. Lueking, C. R. Hatch and P. Ball, Optimization of biofiltration for odor control: Model calibration, validation, and applications, *Water Environment Research* **74**(1) (2002), 17 – 27, DOI: 10.2175/106143002x139712.

[16] S. Raghuvanshi and B. V. Babu, Biofiltration for removal of methyl isobutyl ketone (MIBK): Experimental studies and kinetic modelling, *Environmental Technology* **31**(1) (2010), 29 – 40, DOI: 10.1080/09593330903289705.

[17] E. R. Rene, D. V. S. Murthy and T. Swaminathan, Performance evaluation of a compost biofilter treating toluene vapours, *Process Biochemistry* **40**(8) (2005), 2771 – 2779, DOI: 10.1016/j.procbio.2004.12.010.

[18] M. Sajid and T. Hayat, Comparison of HAM and HPM solutions in heat radiation equations, *International Communications in Heat and Mass Transfer* **36**(1) (2009), 59 – 62, DOI: 10.1016/j.icheatmasstransfer.2008.08.010.

[19] B. Seethalakshmi, V. Ananthaswamy, S. Narmatha and P. F. Shirly, Approximate analytical solution to a pore network model of deactivation of immobilized glucose isomerase in packed-bed reactors using Akbari-Ganji's method, *Communications in Mathematics and Applications* **13**(3) (2022), 865 – 875, DOI: 10.26713/cma.v13i3.1805.

[20] Z. Shareefdeen and B. C. Baltzis, Biofiltration of toluene vapor under steady-state and transient conditions: Theory and experimental results, *Chemical Engineering Science* **49**(24-Part A) (1994), 4347 – 4360, DOI: 10.1016/S0009-2509(05)80026-0.

[21] Z. Shareefdeen, B. C. Baltzis, Y.-S. Oh and R. Bartha, Biofiltration of methanol vapor, *Biotechnology and Bioengineering* **41**(5) (1993), 512 – 524, DOI: 10.1002/bit.260410503.

[22] A.-M. Wazwaz, The variational iteration method for solving linear and nonlinear ODEs and scientific models with variable coefficients, *Central European Journal of Engineering* **4** (2014), 64 – 71, DOI: 10.2478/s13531-013-0141-6.

[23] S. M. Zarook and A. A. Shaikh, Analysis and comparison of biofilter models, *Chemical Engineering Journal* **65**(1) (1997), 55 – 61, DOI: 10.1016/s1385-8947(96)03101-4.

[24] K. Zhao, G. Xiu, L. Xu, D. Zhang, X. Zhang and M. A. Deshusses, Biological treatment of mixtures of toluene and *n*-hexane vapours in a hollow fibre membrane bioreactor, *Environmental Technology* **32**(6) (2011), 617 – 623, DOI: 10.1080/09593330.2010.507634.